EARTHQUAKE ANALYSIS OF THE LOWER SAN FERNANDO DAM USING ELASTIC, EQUIVALENT LINEAR AND BOUNDING SURFACE PLASTICITY MODELS.

Dr. Omar al-Farouk S. al Damluji
Assistant Professor and Head
Department of Civil Engineering
University of Baghdad

Asma Y. al-Tae'e
Assistant Instructor
Department of Civil Engineering
University of Baghdad

ABSTRACT

Uncoupled behaviour of a dam under earthquake loading is investigated. Three constitutive models are used:

- The linear-elastic model where soil properties; shear modulus and damping ratio are strains and cycle independent.
- The equivalent linear model where soil properties are strain dependent but cycle independent. The shear modulus tends to decrease as the shear strain increases, while the damping ratio tends to increase as the shear strain increases.
- A non-linear model where soil properties tend to change not only with shear strain but also with the progression of cycles. In this work, the bounding surface model is used.

For these studies, three kinds of numerical integration methods in the time domain are used, namely, Newmark, Wilson-θ and the α-methods with different damping ratios.

In this study, the bounding surface plasticity model visualizes the realistic behaviour of the dam under the dynamic loading rather than the equivalent linear and the elastic linear models.

الخلاصة

تم دراسة التصرف الديناميكي غير المزدوج لسدة ترابية تحت تأثير الأحمال الديناميكية (الهزات الأرضية)..تم استخدام ثلاثة علاقات تكوينية وهي كالآتي:

نموذج المرونة الخطية: لا تعتمد خصائص التربة (معامل القص ونسبة الإخماد) على مقدار الانفعال الحاصل ولا على طبيعة الحمل المسلط.

النموذج الخطي المكافيء: يعتمد كل من معامل القص ونسبة الاخماد على مقدار الانفعال الحاصل، لكنهما لا يعتمدان على طبيعة الحمل المسلط حيث ان معامل القص يقل بزيادة انفعال القص، بينما تزداد نسبة الإخماد بزيادة انفعال القص.

النموذج اللدن اللاخطي: لا تتغير خصائص التربة فقط بتغير انفعال القص لكن ايضاً تتغير بزيادة دورات التحميل وازالة الثقل. لقد اعتمد نموذج السطح المحيط لإجراء هذا التحليل.

في هذه الدراسات، تم استخدام ثلاثة طرق عددية وهي طريقة نيومارك، طريقة-α وطريقة ولسن-θ لنسب إخماد مختلفة.

في هذه الدراسة تم التوصل إلي إن استخدام نموذج السطح المحيط يعطي التصرف الحقيقي للسد تحت الأحمال الديناميكية افضل من استخدام النموذج الخطي المكافئ والنموذج المرن الخطي.

KEY WORDS
Earthquake, linear model, equivalent model, non- linear model.

INTRODUCTION

Sudden ground displacement during earthquakes induces large inertia forces in embankments or dams. As a result, the slope of an embankment is subjected to several cycles of alternating inertia forces. There are several recorded cases that show severe damage or collapse or earth embankment slope failure due to earthquake-induced vibrations [Ambraseys, 1960; Seed, Makdisi, and DeAlba 1978]. The damages include *flow slides* of saturated cohesionless soil slopes and slopes of cohesive soils with thin lenses of saturated sand inside them. Such flow slides are due to liquefaction of saturated sand deposits. Other types of damages include collapse or deformation of dry or dense slopes in sand and also slopes in cohesive soils.

CONSTITUTIVE RELATIONS

Linear Elastic Model

Dynamics has to be used instead of statics when the motions are such that the effect of inertia can not be neglected. In this case, the equation of the conservation of impulse is used, [Singh 1990]:

$$\underset{\sim}{\sigma} = \underset{\approx}{D}\,\underset{\sim}{\varepsilon} + \underset{\approx}{D'}\,\underset{\sim}{\dot{\varepsilon}}$$

in which $\underset{\approx}{D}$ is the elasticity matrix [Molenkamp and Smith 1980]:

$$\underset{\approx}{D} = \begin{bmatrix} \frac{4}{3}G + K & -\frac{2}{3}G + K & 0 \\ -\frac{2}{3}G + K & \frac{4}{3}G + K & 0 \\ 0 & 0 & G \end{bmatrix} \qquad (1)$$

and

$$\left.\begin{aligned} \underset{\sim}{\varepsilon} &= \underset{\approx}{A}\,\underset{\sim}{u} \\ \underset{\sim}{\dot{\varepsilon}} &= \underset{\approx}{A}\,\underset{\sim}{\dot{u}} \end{aligned}\right\} \qquad (2)$$

$$\underset{\approx}{A} = \begin{bmatrix} \frac{\partial}{\partial x_1} & 0 & 0 \\ 0 & \frac{\partial}{\partial x_2} & 0 \\ 0 & 0 & \frac{\partial}{\partial x_3} \\ \frac{\partial}{\partial x_2} & \frac{\partial}{\partial x_1} & 0 \\ 0 & \frac{\partial}{\partial x_3} & \frac{\partial}{\partial x_2} \\ \frac{\partial}{\partial x_3} & 0 & \frac{\partial}{\partial x_1} \end{bmatrix} \qquad (3)$$

in which $\underset{\approx}{A}$ is the differential operator.

$$\underset{\approx}{D'} = \frac{2G\bar{\xi}}{\omega_n} \begin{bmatrix} \frac{4}{3} & -\frac{2}{3} & 0 \\ -\frac{2}{3} & \frac{4}{3} & 0 \\ 0 & 0 & 1 \end{bmatrix} \qquad (4)$$

in which:

ξ = damping ratio, ω_n = natural frequency, K = bulk modulus (the elastic parameter),
K′ = viscous bulk modulus, G = shear modulus (the elastic parameter),
G′ = viscous shear modulus, σ = stress tensor component,
ε = strain tensor component, $\dot{\varepsilon}$ = strain rate.

Equivalent Linear Model

Vertical propagation of shear waves through the system shown in **Fig. (1)** will cause only horizontal displacements [Schnable, Lysmer, and Seed 1972]:

$$u(x,t) = \overset{*}{E}e^{i(\overset{*}{k}x+\omega t)} + \overset{*}{F}e^{-i(\overset{*}{k}x-\omega t)} \qquad (5)$$

The shear stress on a horizontal plane is:

$$\tau(x,t) = G\frac{\partial u}{\partial x} + \bar{\eta}\frac{\partial^2 u}{\partial x \partial y} = G^*\frac{\partial u}{\partial x} \qquad (6)$$

$$= i\overset{*}{k}G^*(\overset{*}{E}e^{i\overset{*}{k}x} - \overset{*}{F}e^{-i\overset{*}{k}x})e^{i\omega t} \qquad (7)$$

$$\gamma = \frac{\partial u}{\partial x} = i\overset{*}{k}(\overset{*}{E}e^{i(\overset{*}{k}x+\omega t)} - \overset{*}{F}e^{-i(\overset{*}{k}x-\omega t)}) \qquad (8)$$

where:

E,F = constants, $\overset{*}{k}$ = complex wave number, G^* = complex shear modulus,
τ = shear stress, γ = shear strain, and t = time.

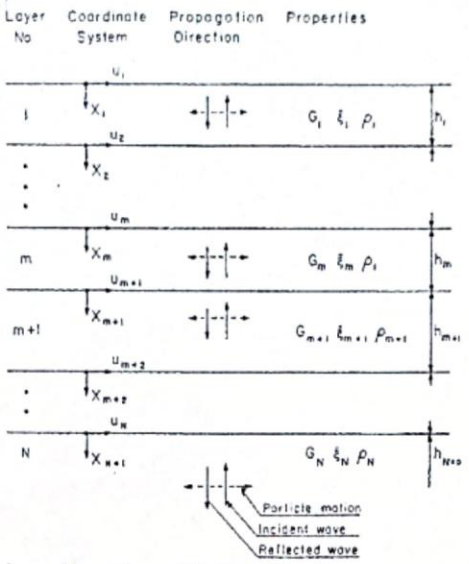

Fig.(1) One- dimensional system [Schnable, Lysmer, and Seed 1972]

Non-Linear (Plasticity) Model

The stress- strain rate relationship for elastoplasticity state can be expressed by [Kaliakin and Herrmann 1989]:

$$\dot{\sigma}_{ij} = D_{ijk\ell}\dot{\varepsilon}_{k\ell} \qquad (9)$$

where:

$$D_{ijk\ell} = \left[2G\delta_{ik}\delta_{j\ell} + \left(K - \frac{2}{3}G\right)\delta_{ij}\delta_{k\ell}\right] - \left\{3KF_{,\bar{I}}\,\delta_{k\ell} + \frac{G}{J}F_{,\bar{J}}\,s_{k\ell} + \frac{\sqrt{3}GF_{,\bar{\alpha}}}{bJ\cos 3\bar{\alpha}}\left[\frac{1}{J^2}\left(s_{kn}s_{n\ell} - \frac{3}{2}\frac{S^3}{J^2}s_{k\ell}\right) - \frac{2}{3}\delta_{k\ell}\right]\right\} \times \left\{3KF_{,\bar{I}}\,\delta_{ij} + \frac{G}{J}F_{,\bar{J}}\,s_{ij} + \frac{\sqrt{3}GF_{,\bar{\alpha}}}{bJ\cos 3\bar{\alpha}}\left[\left[\frac{1}{J^2}\left(s_{in}s_{nj} - \frac{3}{2}\frac{s^3}{J^2}s_{ij}\right) - \frac{2}{3}\delta_{ij}\right]\right\}\frac{\mathscr{L}}{D} \qquad (10)$$

$$\mathscr{L} = \begin{cases} 1 & \text{if } L > 0 \\ 0 & \text{if } L \le 0 \end{cases} \qquad (11)$$

$$D = K_p + 9K(F_{,\bar{I}})^2 + G\left[(F_{,\bar{J}})^2 + \left(\frac{F_{,\bar{\alpha}}}{bJ}\right)^2\right] \qquad (12)$$

RESULTS

Linear Elastic Model

One-dimensional analysis:

In a dynamic analysis, a column of soil is subjected to a low frequency sinusoidal load at the top surface. The properties of the soil are shown in **Table (1)** [Pande and Zienkiewicz 1982]. The mesh of the column is shown in **Fig. (2)**.

Table (1) The properties of the soil column, [Pande and Zienkicwicz 1982].

Material zone		Dynamic Elastic modulus (MN/m^2)	Dynamic Poisson's ratio (ν)	Density (kg/m^3)
1	Alluvium	200	0.4	2090
2	Hydraulic fill sand	90	0.41	2020
3	Clay core	43.092	0.35	1800

The results of the displacements and the stress- strain relationships are shown in **Figs. (3a) and (3b)**. From **Fig (3a)** , it can be seen that the maximum displacement is 0.687 while from **Fig (3b)**, the behaviour of the stress- strain relationship is linear.

Sinusoidal load with ω = 2 rad/sec.

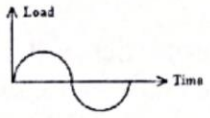

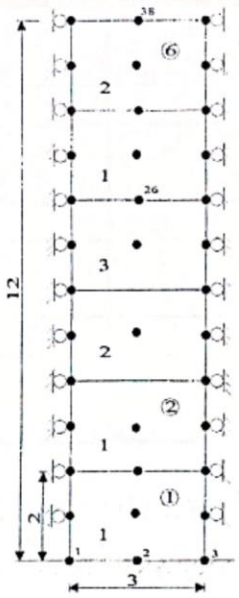

Fig. (2) The mesh of the column of soil (dimensions are in meters).

Only under a very light loading, the soil behaves as a linear elastic material.

Two-dimensional analysis:

In a dynamic analysis, the Lower San Fernando Dam is subjected to the San Fernando earthquake with a maximum base acceleration of 5.53 m/sec^2. This problem has been adopted because of availability of required data for analysis. The adopted properties of the dam are shown in **Table (2)**. The problem is discretized as shown in **Fig. (4)**. The mesh consists of (65) elements with (297) nodes. The dam is constructed from different materials see **Table (2) and Fig. (4b)**. The core of the dam is clay, the sides of the core are constructed from the hydraulic fill sand material and the top of the dam is constructed from the ground shale- hydraulic fill and rolled fill materials.

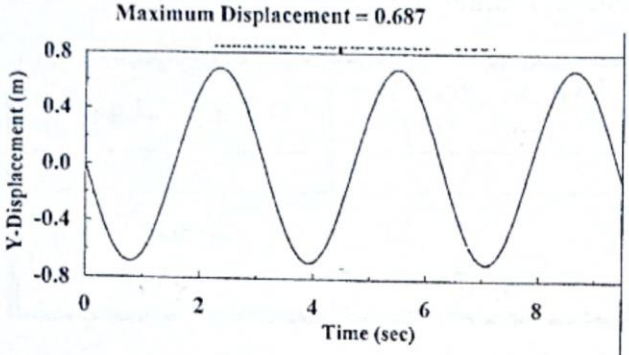

Fig. (3a) Displacement response at node 26. (α- Method, Boundary condition: Fixed- Free, $\bar{a} = 0.05$, $\bar{b} = 0.0003$)

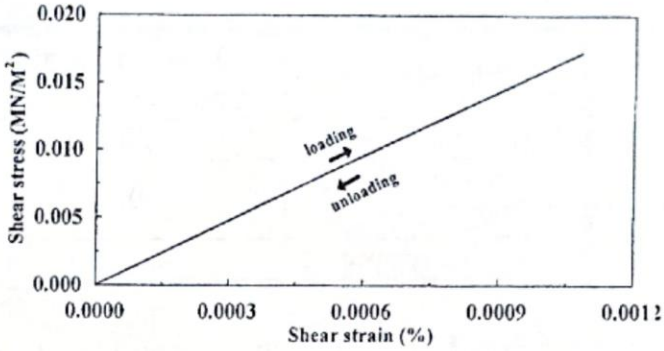

Fig. (3b) Stress-strain relationship for element = 4. (α- Method, Boundary condition: Fixed- Free, $\bar{a} = 0.05$, $\bar{b} = 0.0003$)

Table (2) The assumed properties of the Lower San Fernando Dam, [Pande and Zienkicwicz 1982].

Material zone		Dynamic Elastic modulus (MN/m^2)	Dynamic Poisson's ratio (ν)	Density (kg/m^3)
1	Alluvium	200	0.4	2090
2	Hydraulic fill-sand	90	0.41	2020
3	Clay core	90	0.41	2020
4	Hydraulic fill-sand	110	0.41	2020-sat. 1710-dry
5	Rolled fill	60	0.3	2000
6	Ground shale-Hydraulic fill	90	0.41	2020-sat. 1710-dry

Without consideration of the action of the water at the upstream side:

The results of the displacements and stress-strain relationship are displayed for only two locations at the dam. One is at the top and the other at the bottom. These calculations are made for different time integration schemes (Newmark method, α-method and Wilson-θ method), different damping ratios and for different boundary conditions. The results are shown in **Table (3)** and **Fig. (5)**.

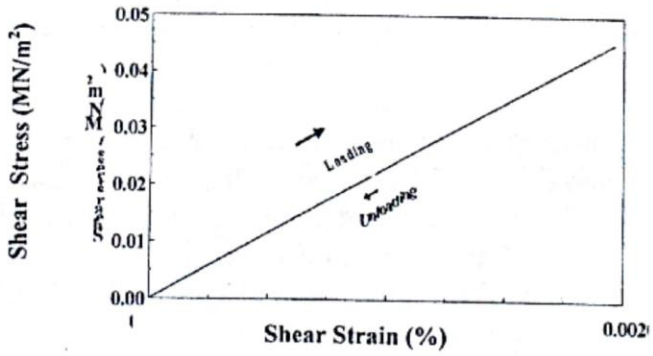

Fig.(5) Stress-strain relationship for element = 65.

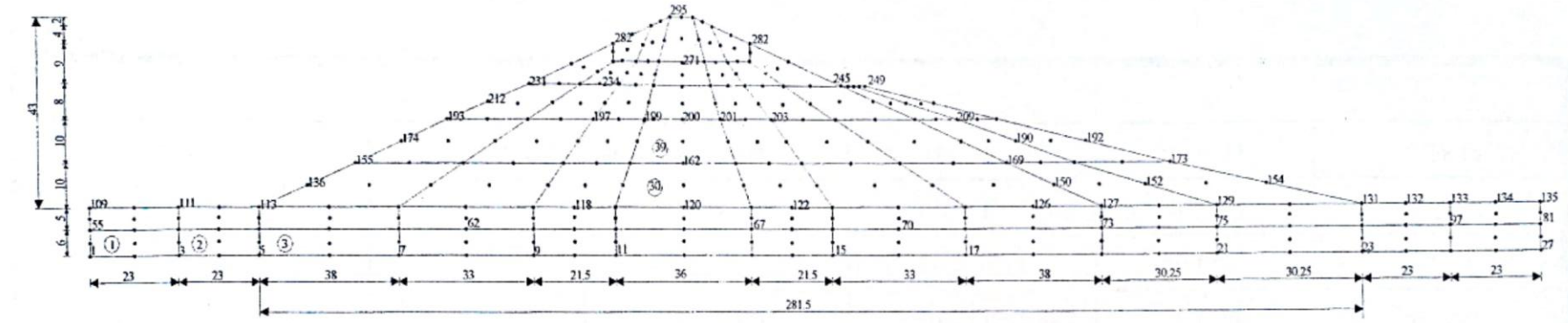

(a)

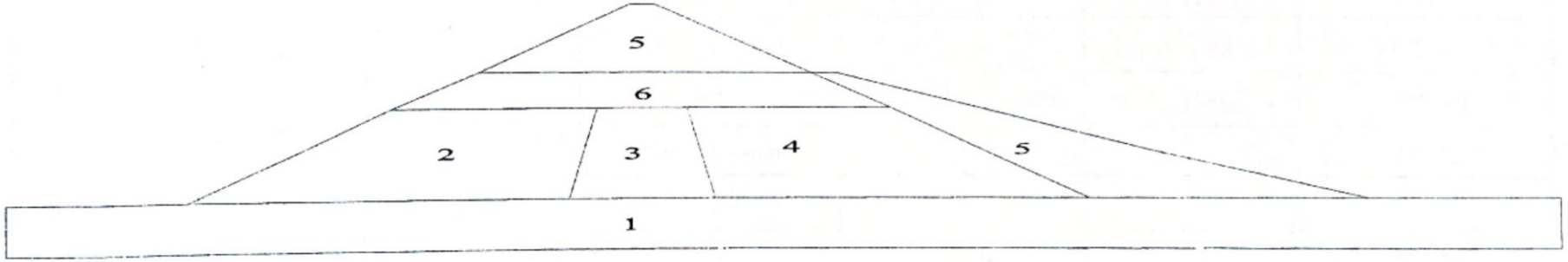

(b)

Fig. 4 (a) The Input Mesh of the Analysis for the Lower San Fernando Dam and (b) the Material Type Numbers of the Cross-Section (Dimensions are in Meters) [Pande and Zienkicwicz 1982].

Table (3) Displacement response for many locations at the dam under the linear model

Reservoir	Node	Boundary condition	Method	Damping	X-Displacement (m)	Y-Displacement (m)
Without consideration of the action of water	295	Fixed- Free	Newmark method	$\bar{a} = 0$, $\bar{b} = 0$	-0.3036	-0.2757
			α- method		-0.2530	-0.2750
			Wilson-θ method		-0.3019	-0.2842
			Newmark method	$\bar{a} = 0.05$, $\bar{b} = 0.0003$	-0.2995	-0.2757
			α- method		-0.2240	-0.2730
			Wilson-θ method		-0.2988	-0.2841
			Newmark method	$\bar{a} = 0.05$, $\bar{b} = 0.003$	-0.2627	-0.2756
			α- method		-0.2240	-0.2730
			Wilson-θ method		-0.2717	-0.2833
			Newmark method	$\bar{a} = 0.5$, $\bar{b} = 0.03$	-0.1794	-0.2670
			α- method		-0.1630	-0.2660
			Wilson-θ method		-0.1829	-0.2758
		Free- Free	α- method	$\bar{a} = 0.05$, $\bar{b} = 0.003$	-0.1960	-0.4300
	113	Fixed- Free	Newmark method	$\bar{a} = 0.05$, $\bar{b} = 0.003$	-0.7651	-0.5844

Table (3) (continued)

Reservoir	Node	Boundary condition	Method	Damping	X-Displacement (m)	Y-Displacement (m)
Without consideration of the action of water	113	Fixed- Free	α- method	$\bar{a} = 0.05$, $\bar{b} = 0.003$	-0.7651	-0.5844
			Wilson-θ method	$\bar{a} = 0.05$, $\bar{b} = 0.003$	-0.7660	-0.5889
		Free- Free	α- method	$\bar{a} = 0.05$, $\bar{b} = 0.003$	-1.048	-0.871
	125	Fixed- Free	α- method	$\bar{a} = 0.05$, $\bar{b} = 0.003$	-0.05206	-0.0333
	157				-0.0814	-0.3433
	159				-0.0556	-0.343
	163				-0.0502	-0.315
	173				-0.0231	-0.322
	193				-0.1400	-0.398
	211				-0.045	-0.207
	237				-0.1883	-0.274
	245				-0.172	-0.2133
Including the action of water	295	Fixed- Free	α- method	$\bar{a} = 0.05$, $\bar{b} = 0.003$	-0.2238	-0.273
	113				-0.7655	-0.585

From these results, the following can be noticed:

1- The difference between Newmark method and Wilson-θ method is very small in x-displacements at the end time of the earthquake but there is some difference in y-displacements at the end time of the earthquake. The difference between Newmark method and α-method is very small in y-displacements but there is some difference in x-displacements. The results of α-method are more realistic than the others when the damping ratio increases.
2- When the damping ratio increases, the displacement response decreases.
3- Two analyses are carried out employing the same numerical method (α-method) and adopting fixed coefficients for damping ratio ($\bar{a}$ = 0.05, $\bar{b}$ = 0.003). In the first analysis, the nodes on the left and right vertical boundary lines of the mesh are considered to be free in the y-direction and constrained in the x-direction. Conversely, in the second analysis, they are considered to be free in both directions. The results of the displacements of the first analysis are greater than the second one in the x-direction, but lower than them in the y-direction.

Including the action of the water at the upstream side:

The hydrodynamic pressure acting on the dam is considered at the upstream face where it is calculated using Zanger's method [Okamoto 1973].

From **Table (3)**, it can be seen that the displacement response when including the action of water is less than that without.

By using the α-method and without considering the action of water, the final deformation shape of the dam is shown in **Fig.(7)**

Equivalent Linear Model

Calculation of the average shear modulus of the Lower Dam:

The average shear modulus of the dam material is estimated from the fundamental period of the dam [Bureau of Reclamation, U.S. Department of the Interior 1986]. Fourier amplitude spectra are calculated for the time-acceleration records at the outcrop and crest of the dam. The amplification spectrum is calculated by dividing the Fourier amplitude of the crest record by the corresponding Fourier amplitude of the outcrop record (the ratio between the amplitude of the base rock motion and the outcropping rock motion is always less than 1 [Schnable, Lysmer, and Seed 1972]). These results are shown in **Fig. (8)**.

Fig. (7) The final form of the Lower San Fernando Dam under the linear model

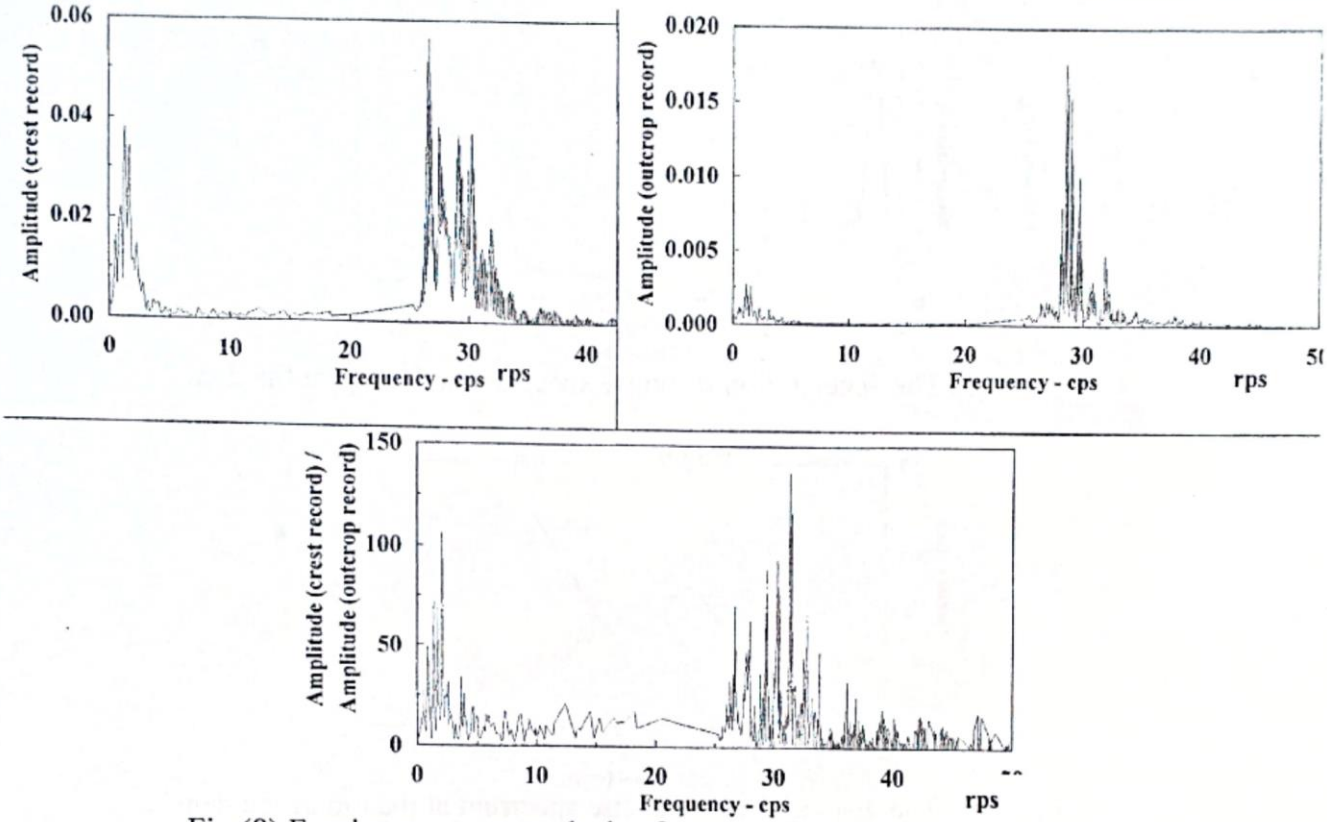

Fig.(8) Fourier spectrum analysis of measured time-acceleration records

Calculation of the effective mass density, shear modulus and viscosity for the dam:

To analyze the Lower Dam by the SHAKE program, the wave equation is converted to [Whiteside, France, and Castro 1979]:

$$\left(\rho_i \frac{L_i}{L_b}\right)\frac{\partial^2 u}{\partial t^2} = \left(G_i \frac{L_i}{L_b}\right)\frac{\partial^2 u}{\partial x^2} + \left(\overline{\eta}_i \frac{L_i}{L_b}\right)\frac{\partial^3 u}{\partial x^2 \partial t} \qquad (15)$$

where:

L_i = the length of layer i,

L_b = the length of the layer representing the base of the dam,

$\left(\rho_i \frac{L_i}{L_b}\right)$ = effective mass density, $\left(G_i \frac{L_i}{L_b}\right)$ = effective shear modulus, and,

$\left(\overline{\eta}_i \frac{L_i}{L_b}\right)$ = effective viscosity.

Figs. (9) and **(10)** show the acceleration response spectrum and displacement response spectrum at the top of the dam.

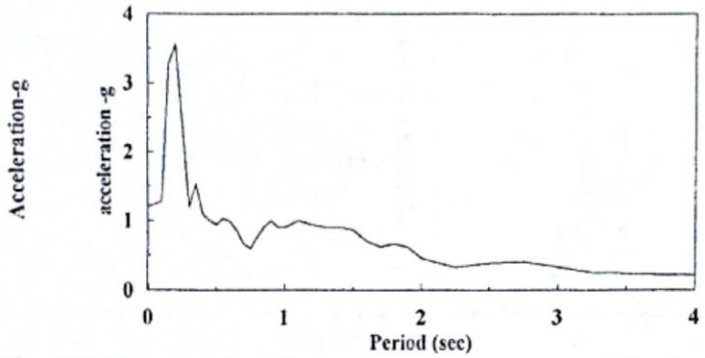

Fig. (9) The acceleration response spectrum at the top of the dam.

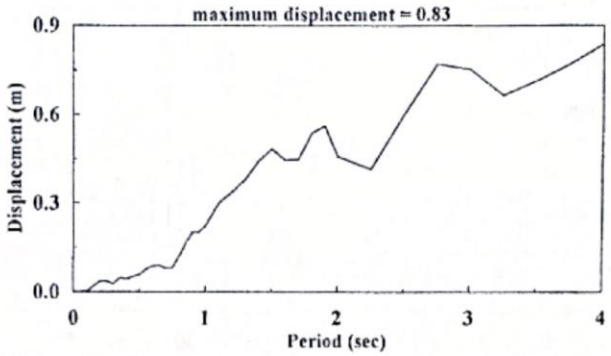

Fig. (10) The displacement response spectrum at the top of the dam.

From **Fig. (10)** and **Table (3)** (node= 295), it can be seen that the horizontal displacement of the linear analysis (0.3036 m) is less than the displacement under the equivalent linear model (0.83 m). This is because of that the properties of the soil under the equivalent linear model are strain dependent.

Non-Linear Model

In this model, the finite element method is used along with the bounding surface plasticity model, as a constitutive relation, to show the behaviour of the soil under an earthquake. A particular soil, Boston Blue clay, is selected.

Boston Blue clay is a low-plasticity (I_p = 19% to 23%), illitic, marine clay of moderate sensitivity that was deposited in Boston basin during the Pleistocene glatiation [Whittle et al 1994]. Engineering properties of Boston Blue clay have been studied extensively and, there is a large data base of reliable tests from which to select all the required input parameters. These parameters were selected from different sources ([Levadoux 1980] and [Whittle et al 1994]). The input parameters for the bounding surface model used in the analyses herein are shown in **Table (4)**.

Table (4) Material properties for the bounding surface model

λ	0.184
κ	0.02
M_c	1.2026
Me/M_c	0.8998
ν	0.35
$I\ell$	30.4
P_{atm}	101.4
R_c	2.3
A_c	0.1
T	0.1
R_e/R_c	0.8
A_e/A_c	0.8
C	0.4
s_p	1
M	0.02
h_c	10
h_e/h_c	1
h_0	10
e_0	1.12
s_v	5
V	1×10^6

One dimensional analysis:

The soil column in **Fig. (2)** is subjected to a low frequency sinusoidal load at the top surface. The displacement response and stress-strain relationship are shown in **Figs. (11)** and **(12)**.

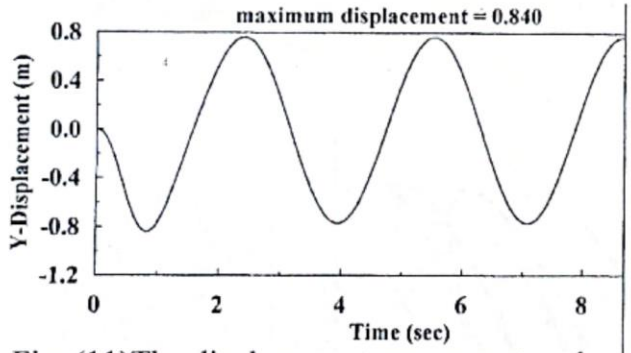

Fig. (11)The displacement response at node =26.
(α- Method, Boundary condition: Fixed-Free, $\bar{a} = 0.05$, $\bar{b} = 0.0003$)

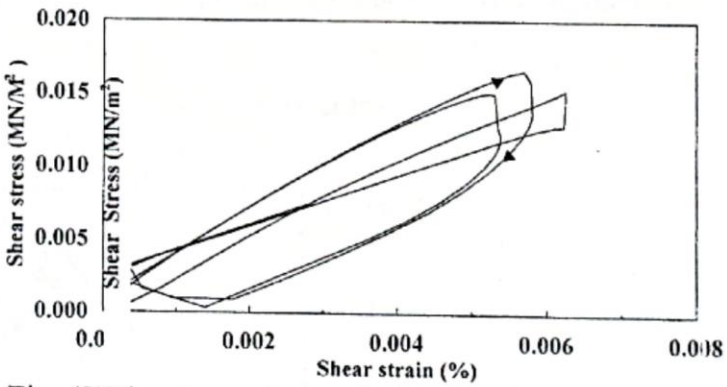

Fig. (2)The stress-strain relationship for element = 4.
(α- Method, Boundary condition: Fixed- Free, $\bar{a} = 0.05$, $\bar{b} = 0.0003$)

In this model, the stress-strain relationship represents the realistic behaviour of the soil under the dynamic loading, as opposed to the elastic-linear and equivalent linear models. Therefore, the use of the bounding surface plasticity model to predict the actual response of the soil under dynamic load is very important.

Two-dimensional analysis:

The dam shown in **Fig.(4)** is subjected to the San Fernando earthquake and the clay core response is investigated by the bounding surface plasticity model. The material properties used are those of the Boston Blue clay representing the clay core of the Lower San Fernando Dam which are shown in **Table (5)**.

Table (5) Material properties of the clay core of Lower San Fernando Dam

Material zone		Dynamic Elastic modulus (MN/m^2)	Dynamic Poisson's ratio v	Density (kg/m^3)
1	Alluvium	200	0.4	2090
2	Hydraulic fill-sand	90	0.41	2020
3	Clay core	43.092	0.35	1806
4	Hydraulic fill-sand	110	0.41	2020-sat. 1710-dry
5	Rolled fill	60	0.3	2000
6	Ground shale-Hydraulic fill	90	0.41	2020-sat. 1710-dry

A few seconds after the beginning of the earthquake, the strain increases exceeding 5%, therefore the dam fails quickly. Because of the replacement of the actual clay core in the dam by a different one, Boston Blue, the dam fails. The displacement response and the behaviour of the soil under the bounding surface model immediately before the occurrence of failure can be shown in **Table (6)** and in **Fig. (13)**.

The same dam is re-analyzed using the same properties and conditions, but water in the reservoir is introduced. **Table (6)** shows the results.

Comparing the results of the two analyses (without and with the consideration of the action of water), it is seen that the difference between them is small.

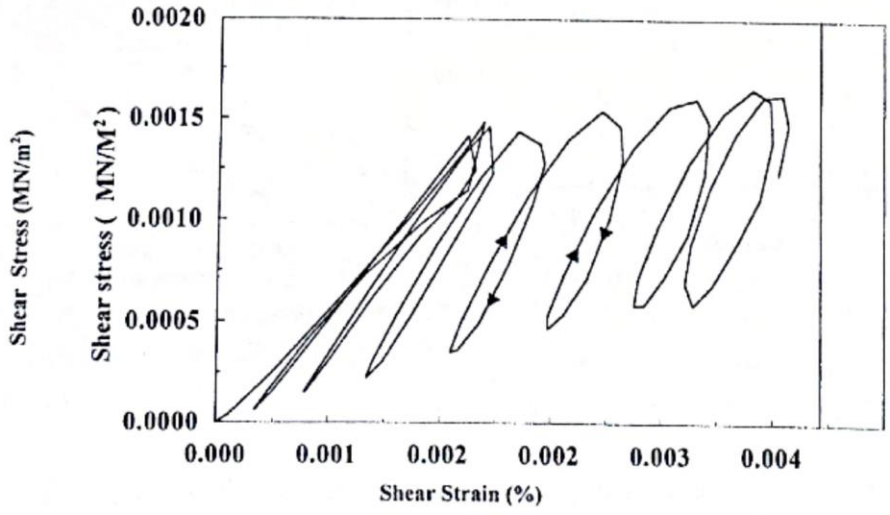

(a)

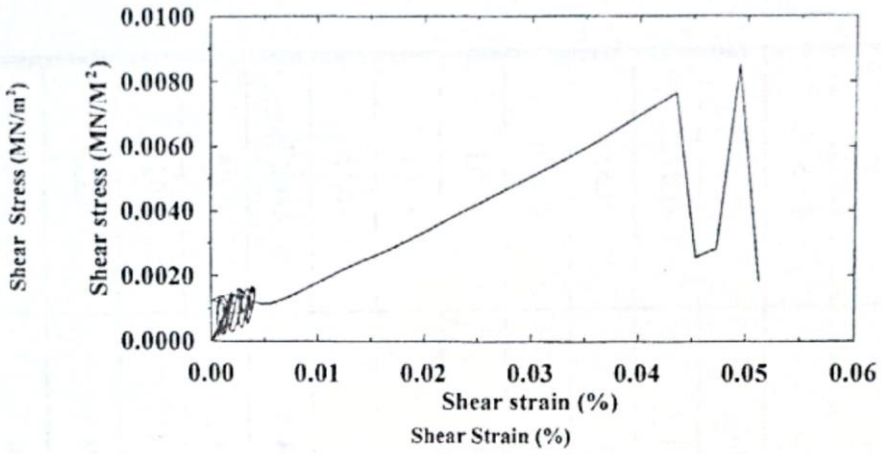

(b)

Fig. (13) Stress-strain relationship for element = 30
(a) at 1 sec (b) at 3 sec

Because the properties of the soil in this model not only change with the shear strain, but also with the progression of cycles, the expected deformation is larger than that of the linear and equivalent linear models. In the bounding surface plasticity model, the dam reaches the failure condition. The shape of the failure is rather similar to the actual failure of the dam because the finite element method incorporated with this constitutive relationship models the problem appropriately. In this analysis, the Newmark method is used as a numerical integration scheme in the time domain to arrive at the solution in **Table (6)**, without the introduction of water in **Fig. (14a)**. This result is compatible with the Cap model reduction [Bureau of Reclamation, U. S. Department of the Interior, 1986] see **Fig. (14b)**.

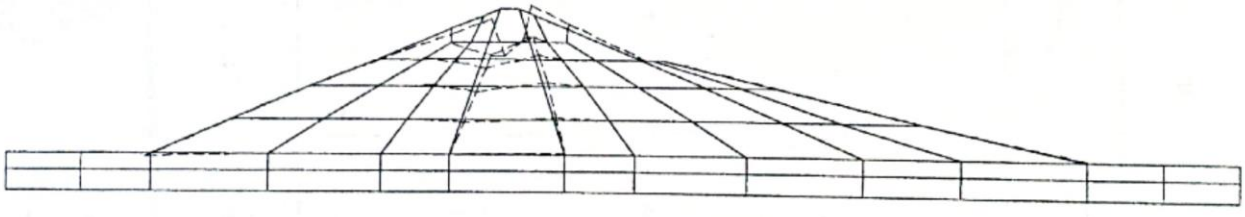

(a)

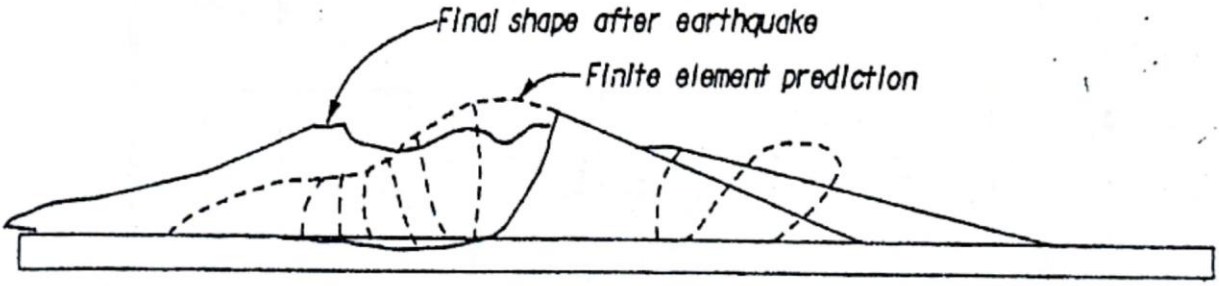

(b)

Fig. (14 a) The final form of the Lower San Fernando Dam under the bounding surface model (b) The final form of the Lower San Fernando Dam under the cap model, [Bureau of Reclamation, U.S. Department of Interior 1986]

Table (6)
Displacement response for many locations at the dam under the bounding surface model

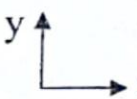

Reservoir	Node	Boundary condition	Method	Damping	X-Displacement (m)	Y-Displacement (m)
Without consideration the action of water	295	Fixed- Free	Newmark method	$\bar{a}=0,\ \bar{b}=0$	2.20	-13.8
	113				1.46	-0.927
	125				0.21	-0.072
	157				0.40	0.53
	159				0.18	-0.096
	163				0.15	-0.03
	173				0.39	0.15
	193				0.93	-2.13
	211				0.04	-0.027
	237				0.14	-0.05
	245				0.014	-0.025
Including the action of water	295	Fixed- Free	Newmark method	$\bar{a}=0,\ \bar{b}=0$	2.19	-13.8
	113				1.46	- 0.927

CONCLUSIONS

The following conclusions have been reached:

1- The differences among the methods of direct integration in the time domain are small.
2- When the damping ratio increases, the α- method is the best numerical integration method for the analysis.
3- When the damping ratio increases, the displacement response decreases.
4- For the linear analysis, the final shape of the deformation is similar to the shape of the actual failure of the dam and in its direction.
5- For the equivalent linear analysis, the peak strain amplitude bears very little relation to the overall level of deformation.
6- Non linear analysis gives strains larger than the linear and the equivalent linear models.
7- It is not easy to deal with the non-linear model. In case of employing the bounding surface plasticity model, the location and shape of the clay core play an important role in obtaining stability of the dam.
8- The non-linear analysis technique is the most realistic algorithm among the others, because it involves the realistic behaviour of soils.

REFERENCES

Al-Assady, A. M., (1998), Effect of Anisotropy on Two-Dimensional Consolidation of Clayey Soil , M.Sc. Thesis, University of Baghdad, Iraq,.

Al-Sarraf, M. A. H., (1999), Cone Penetration in Clay , M.Sc. Thesis, College of Engineering, University of Baghdad,.

Ambraseys, N. N., (1993), On the Seismic Behaviour of Earth Dams , Proceeding, 2nd World Conference on Earthquake Engineering, Tokyo, Vol. 1, PP. 331-345, 1960, as cited by Das,.

Bureau of Reclamation, U.S. Department of Interior, (1986), Dynamic Effective Stress Finite Element Analysis of Dams Subjected to Liquefaction , December,.

Gazetas, G., Debchaudhury, A., and Gasparini, D. A., (1982), Stochastic Estimation of the Nonlinear Response of Earth Dams to Strong Earthquakes , Soil Dynamics and Earthquake Engineering, Vol.1, No.1,.

Kaliakin, V. N., and Herrmann, L. R., (1989), Guidelines for Implementing the Elastoplastic-Viscoplastic Bounding Surface Model for Isotropic Cohesive Soils , University of California, Davis,.

Levadoux, J. N., (1980), Pore Pressure in Clays Due to Cone Penetration , Ph.D. Thesis, MIT Cambridge.

Molenkamp, F., and Smith, M., (1980), Hysteretic and Viscous Material Damping , International Journal for Numerical and Analytical Methods in Geomechanics, Vol.4, pp.293-311,.

Okamoto, S., (1973), Introduction to Earthquake Engineering , University of Tokyo Press,.

Pande, G.N., and Zienkiewicz, O. C., (1982), Soil Mechanics- Transient and Cyclic Loads , John Wiley & Sons,.

Schnable, P. B., Lysmer, J., and Seed H. B., (1972), SHAKE, a Computer Program for Earthquake Response Analysis of Horizontally Layered Sites , Report No. EERC 70-12, Earthquake Engineering Research Center, University of California, Berkeley, December.

Seed, H. B., Makdisi, F. I., and De Alba, P., (1978), Performance of Earth Dams During Earthquakes , Journal of the Geotechnical Engineering Division, ASCE, Vol.104, No. GT7, PP.967-994,.

Singh, D. S., (1990), Theory of Plasticity , Khanna Publishers, Second Edition,.

Whiteside, S. L., France, J. W., and Castro, G., (1986), "Report on Dynamic Analysis of La Fortuna Dam , Volumes 2 and 5, Geotechnical Engineers, Inc., 1979, as cited by Bureau of Reclamation, U.S Department of Interior,.

Whittle, A. J., Degroot, D. J., Ladd, C. C., and Seah, T. H., (1994), Model Prediction of Anisotropic Behaviour of Boston Blue Clay , Journal of Geotechnical Engineering, Vol.120, No. 1, pp.199-224,

ABBREVIATIONS

ASCE: American Society of Civil Engineers.